Electronic Supplementary Material (ESI) for Analyst

Correlation of Surface-enhanced Raman Spectroscopy and Laser Desorption-Ionization Mass Spectrometry Acquired from Silver Nanoparticle Substrates

Bei Nie[a,c*], Rachel N. Masyuko[a] and Paul W. Bohn[a,b,c]

[a] Department of Chemistry and Biochemistry, [b] Department of Chemical and Biomolecular Engineering and [c] Advanced Diagnostics and Therapeutics Initiative, University of Notre Dame, Notre Dame, IN 46556. Fax (574) 631-8366; Tel (574) 631-1649; Email: bnie@nd.edu

***Raman spectrum of p-aminothiophenol* (*p-ATP*).** In order to assign Raman vibration bands correctly, a positive control was carried out utilizing bulk *p*-ATP powder placed on a glass slide under conditions identical to SERS measurements, but without Ag NPs. Figure S1 shows a comparison of Raman and SERS on the same intensity scale. Briefly, in the SER spectrum new peaks at 1391 and 1440 cm^{-1}, marked by (*) in the figure, are assigned to b_2 vibrational modes, ν_{19b} and ν_3, respectively, that are enhanced by charge transfer (CT) from the metal to the LUMO of *p*-ATP.[1,2] These bands are assigned to a CT interaction, because: (a) they are absent in the normal Raman spectrum of solid *p*-ATP; (b) electronic spectra identify the π^* b_2 electronic state as the LUMO into which charge transfer occurs; and (c) the pattern of b_2 mode enhancement follows a vibronic pattern.[3] In addition, the S-H stretch near 2600 cm^{-1} observed in the normal Raman spectrum is completely absent in SERS measurement, consistent with the formation of a deprotonated Ag-S linkage. The detailed nature of the deprotonation product is not known, however one plausible explanation posits dimerization of *p*-ATP to 4,4′-dimercaptoazobenzene (DMAB), leading to the presence of these b_2 vibrations,[4] and indeed ions at *m/z* 248, consistent with DMAB, are observed by mass spectrometry.

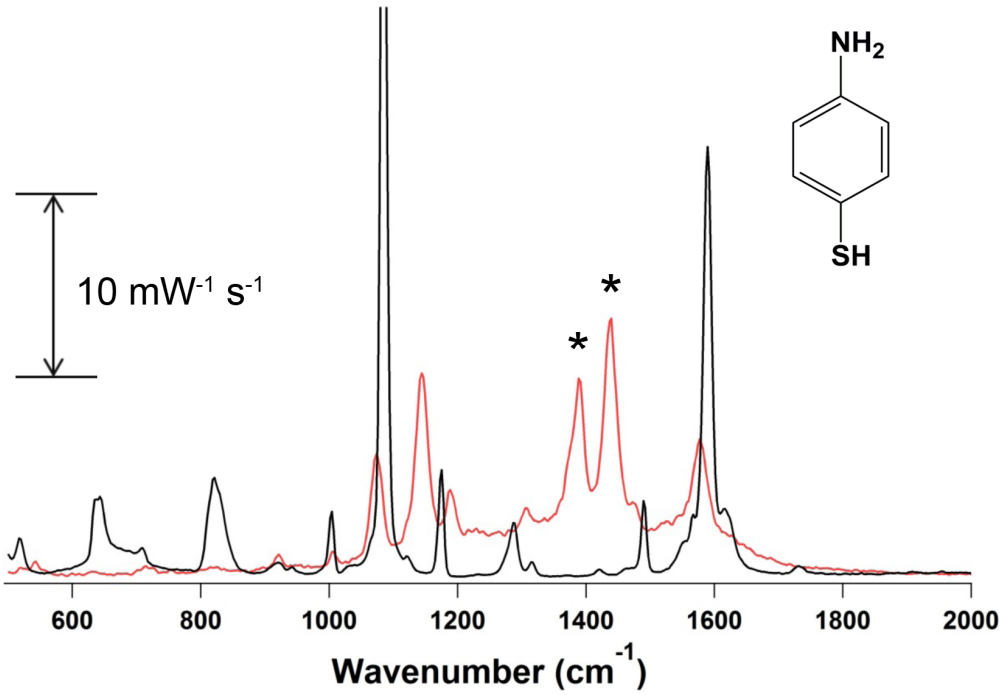

Figure S1. Confocal SERS (red trace) and normal Raman (black trace) spectra of *p*-ATP. SERS spectrum is obtained from a self-assembled monolayer on 20 nm Ag NP/ITO substrate, and normal Raman scattering from bulk *p*-ATP. (*Inset*) Structure of ATP.

Proposed ionization mechanism. Scheme 1 of the main document illustrates the proposed ionization mechanism of *p*-ATP on silver NPs. Both Ag adducts (*m/z* 231,233) and mass-deficient ATP ions (*m/z* 124) are observed in the LDI mass spectrum in Fig. 2(a). The unit mass defect is consistent with the loss of H when forming the Ag-S bond, with the resulting mass-deficient ion formed from dissociation of $[AgATP\text{-}H]^+$. Intriguingly cluster ions of the general formula $[Ag_nATP_m]^+$ are also observed. For example, a multiplet spanning the range m/z 586 - 593 with unit mass offset can be assigned to clusters with (*n*,*m*) = (2,3), where the observed ions arise from ^{107}Ag and ^{109}Ag combining with either regular (*m/z* 125) or mass deficient (*m/z* 124) ATP molecular ion, *viz.* Fig. S2 and Table S1.

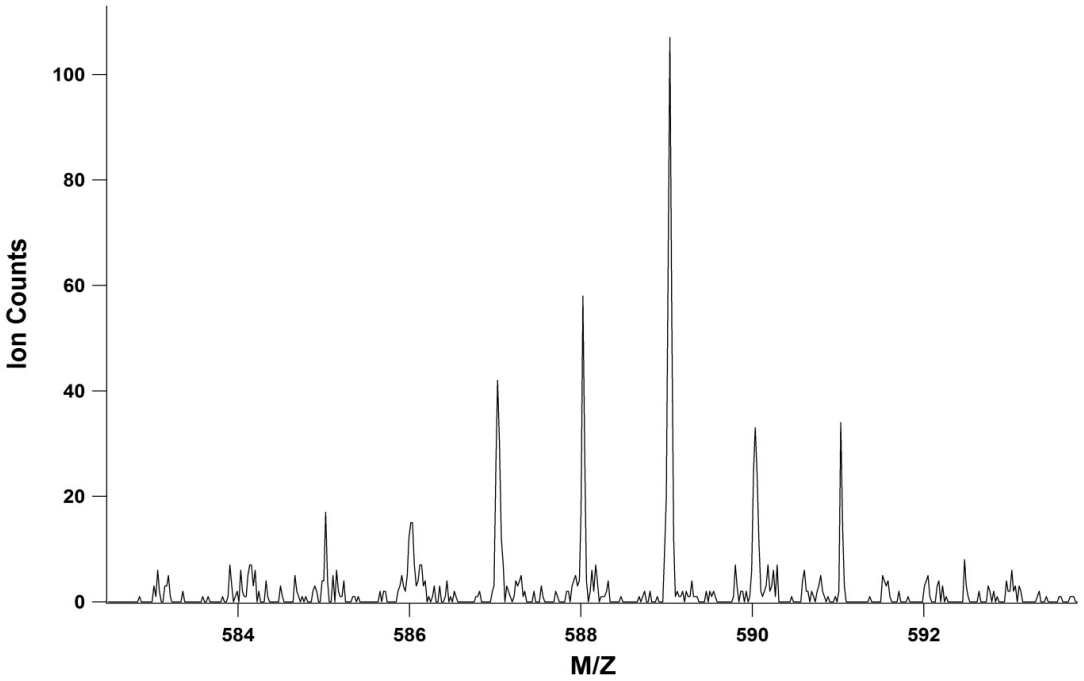

Figure S2. LDI-MS of Ag-ATP mixed cluster ions near *m/z* 589, which shows an ion multiplet with unit mass shift. The mass assignments are given in Table S1.

Cluster Ion	**Molecular Mass**
$[ATP]^+$, $[ATP\text{-}H]^+$	*m/z* 125, 124
$[^{107}Ag_2{}^{124}ATP_3]^+$	*m/z* 586
$[^{107}Ag_2{}^{124}ATP_2{}^{125}ATP]^+$	*m/z* 587
$[^{107}Ag^{109}Ag^{124}ATP_3]^+$	*m/z* 588
$[^{107}Ag_2{}^{124}ATP^{125}ATP_2]^+$	*m/z* 588
$[^{107}Ag^{109}Ag^{124}ATP_2{}^{125}ATP]^+$	*m/z* 589
$[^{107}Ag_2{}^{125}ATP_3]^+$	*m/z* 589
$[^{109}Ag_2{}^{124}ATP_3]^+$	*m/z* 590
$[^{107}Ag^{109}Ag^{124}ATP^{125}ATP_2]^+$	*m/z* 590
$[^{109}Ag_2{}^{124}ATP_2{}^{125}ATP]^+$	*m/z* 591
$[^{107}Ag^{109}Ag^{125}ATP_3]^+$	*m/z* 591
$[^{109}Ag_2{}^{124}ATP^{125}ATP_2]^+$	*m/z* 592
$[^{109}Ag_2{}^{125}ATP_3]^+$	*m/z* 593

Table S1. Detailed compositions of possible $[Ag_2ATP_3]^+$ mixed cluster ions.

MS analysis of R6G$^+$. To further verify the resulting MS spectra from Ag NP based ionization, an ethanolic R6G·HCl solution (1μM) was analyzed by both regular MALDI and electrospray mass spectrometry. In the MALDI experiment, 1μL of 1μM R6G·Cl was mixed with 1μL of 10 mg/mL DHB in methanol. The resulting mixture was then deposited on an ITO slide and allowed to dry. The MALDI-MS spectra were acquired on a Bruker-Dalton Autoflex III MALDI-TOF-TOF equipped with a frequency-tripled Nd:YAG laser producing 355 nm pulses at 100 Hz. The mass spectrometer was set to: reflection mode with 20kV accelerating voltage, acquisition range from 60 to 1600 m/z, spectrum integrated over 200 laser shots, laser fluence ~50 mJ cm^{-2}. The resulting data were recorded and analyzed by software (Autoflex Analysis) provided by the Bruker-Dalton. All data were digitally exported and reconstructed using Igor Pro 6.1 (Lake Oswego, OR). The electrospray MS analysis was performed on a Thermo LTQ LX ion trap mass spectrometer. The sample was infused via syringe pump at 3μL min^{-1}. The mass spectrometer was set to: source voltage 5.0 kV; source current 3.2 μA; full scan range 150-1500 *m/z*. Figure S3 exhibits the resulting MALDI-MS and ESI-MS of R6G. These spectra clearly show the protonated free base, $[R6G+H]^+$ (*m/z* 443.5) obtained upon dissolution of the hydrochloride. Clearly, the protonated free base is the expected species under ESI conditions, and this ion also dominates the MALDI spectrum, rather than the nominal molecular ion at *m/z* 481.

Additional Analytes. In order to explore the connection between LDI and SERS further, complementary spectra were acquired for glucose and retinol, and LDI-MS were acquired for 1,2-dilinoleoyl-sn-glycero-3-phosphocholine and angiotensin (not shown). Data are given in Figs. S4-6, respectively. Glucose (Fig. S4) was chosen, because of its biomedical relevance and because it is a challenging, but tractable, compound to assay with Ag nanostructures. The Ag NP LDI-MS of glucose is dominated by a Ag-glucose adduct peak at *m/z* 299/301, 12 Da higher than the Ag-molecular ion (287/289). The isotopic distribution identifies it as a single Ag atom adduct and its molecular weight indicates a likely origin as a fragment of a higher mixed cluster, $[AgGlu_2\text{-}X]^+$. The SERS spectrum of 100

picomoles of glucose dropcast onto a Ag NP surface is shown in Fig. S4(b) and is compared to the normal Raman spectrum of glucose powder. The SERS spectrum obtained from the LDI-MS active surface is clearly in good agreement with the normal Raman spectrum of the bulk material, an important observation given the recently demonstrated application of SERS to glucose monitoring.[5]

Proceeding to higher molecular weight components, retinol was chosen for the generic importance of the retinoid family of compounds and the commercial importance of retinol, in particular. It (Fig. S5) gives clean LDI-MS spectra from Ag NP substrates, but it does not exhibit a Ag-molecular ion adduct, showing several different Ag-fragment adducts instead. It shows an interesting mass distance (Δm/z 84/86) between the sodium adduct and the corresponding Ag-adducts (doublet), indicating that both Na^+ and Ag^+ add to the same fragment. Consistent with the behavior of glucose its Raman spectrum is strong from the LDI substrate with an interesting alteration from the spectrum of the native compound.[6] A strong, broad band near 1340 cm^{-1} corresponds to a degradation product observed by Failloux *et al.* (1336 cm^{-1}) under uv irradiation. Given the uv liability of the retinoid the appearance of the peak is not surprising especially given the possibility that its generation might be enhanced by the presence of the Ag NPs.

Proceeding higher yet in molecular weight, 1,2-dilinoleoyl-sn-glycero-3-phosphocholine (Fig. S6) does not give a molecular ion adduct either, although the presence of a strong peak at *m/z* 86 suggest facile cleavage of a quaternary ammonium fragment in the presence of Ag. The correlated SERS spectrum from 200 picomoles of phosphatidylcholine is illustrated in Fig. S6(b) compared to the normal Raman spectrum of the bulk crystal as a positive control. Although the SERS spectrum of 1,2-dilinoleoyl-sn-glycero-3-phosphocholine has not been reported to our knowledge, the spectrum compares well both with the normal Raman spectrum of the powder, after allowing for red shifts due to surface interations and with the SERS mediated spectrum of 1,2-[d62]-dipalmitoyl-sn-glycero-3-phosphocholine reported by Leverette and Dluhy.[7]

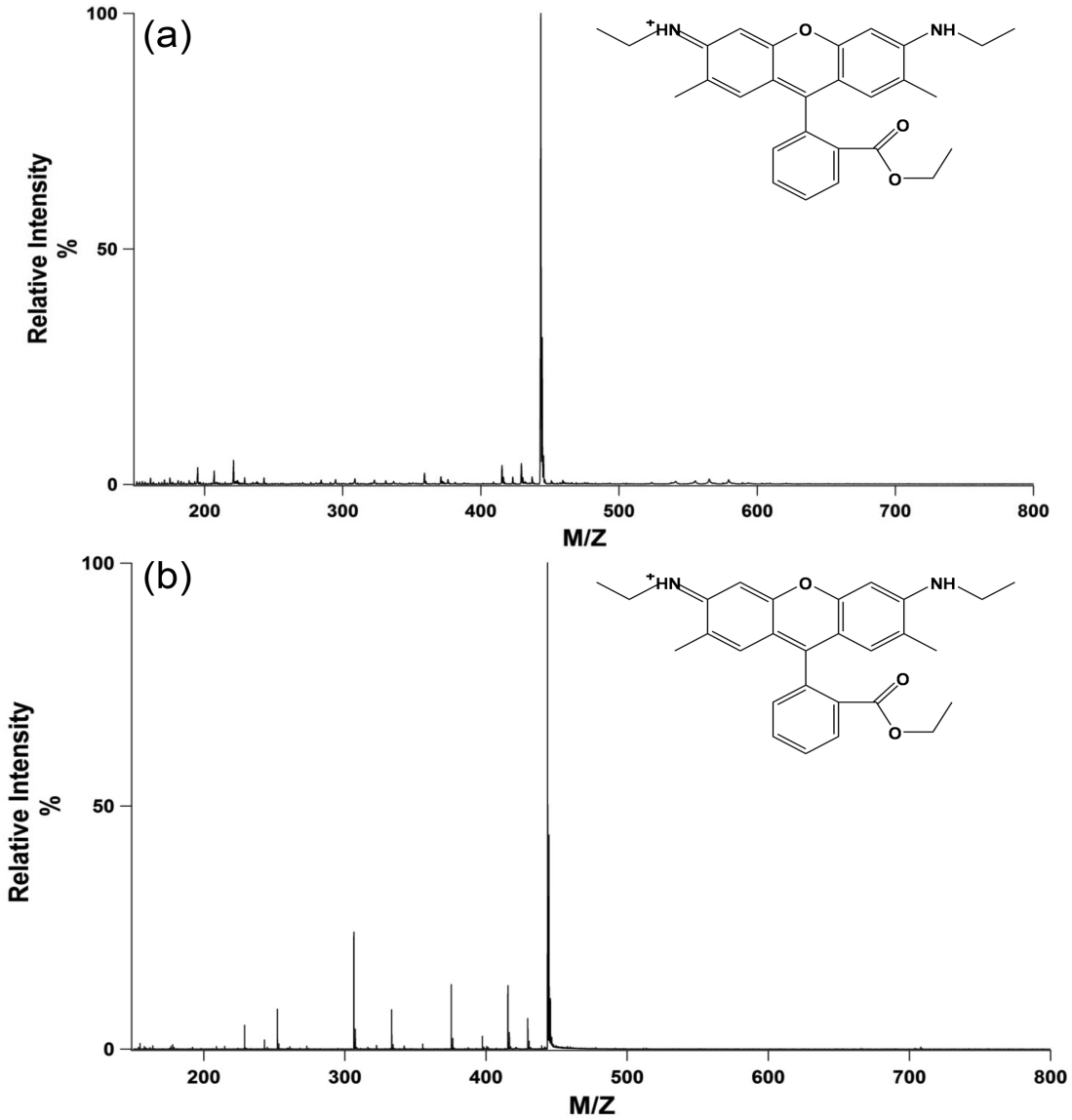

Figure S3. (a) ESI-MS of 1 µM R6G. (b) MALDI MS of 1 µM R6G using 10mg/mL DHB as matrix. Both spectra exhibit the protonated free base at m/z 443.5.

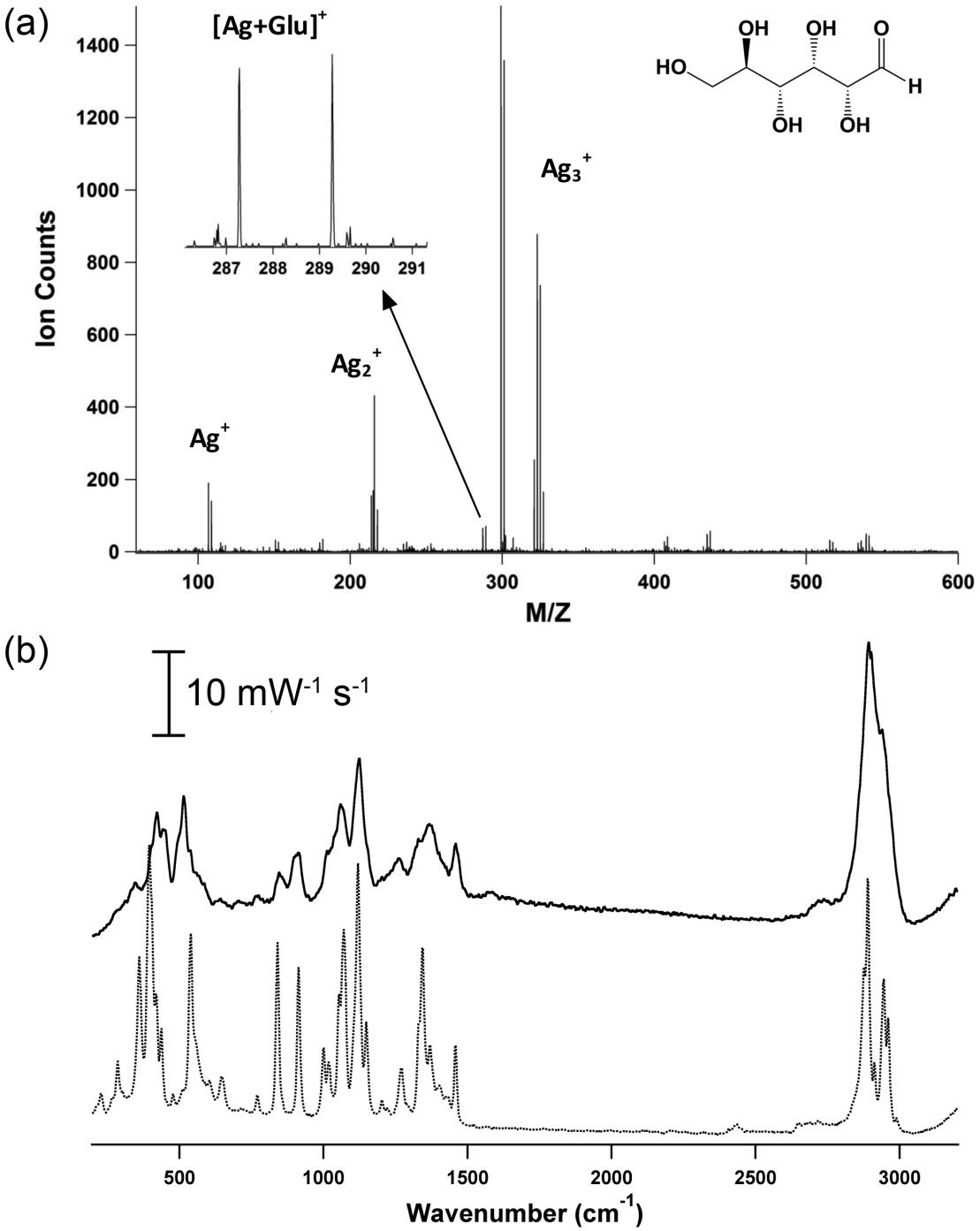

Figure S4. (a) LDI-MS of 100 pmoles of glucose from Ag NP surface. (*Inset*) Magnified MS peak at *m/z* 287/289, assigned to $[Ag+Glu]^+$. The intense peak at m/z 299/301 is posited to be a Ag adduct of a higher fragment. (b) The corresponding SERS (solid) spectrum of 100 µM glucose dropcast onto a Ag NP substrate compared to the normal Raman spectrum of glucose powder (dashed).

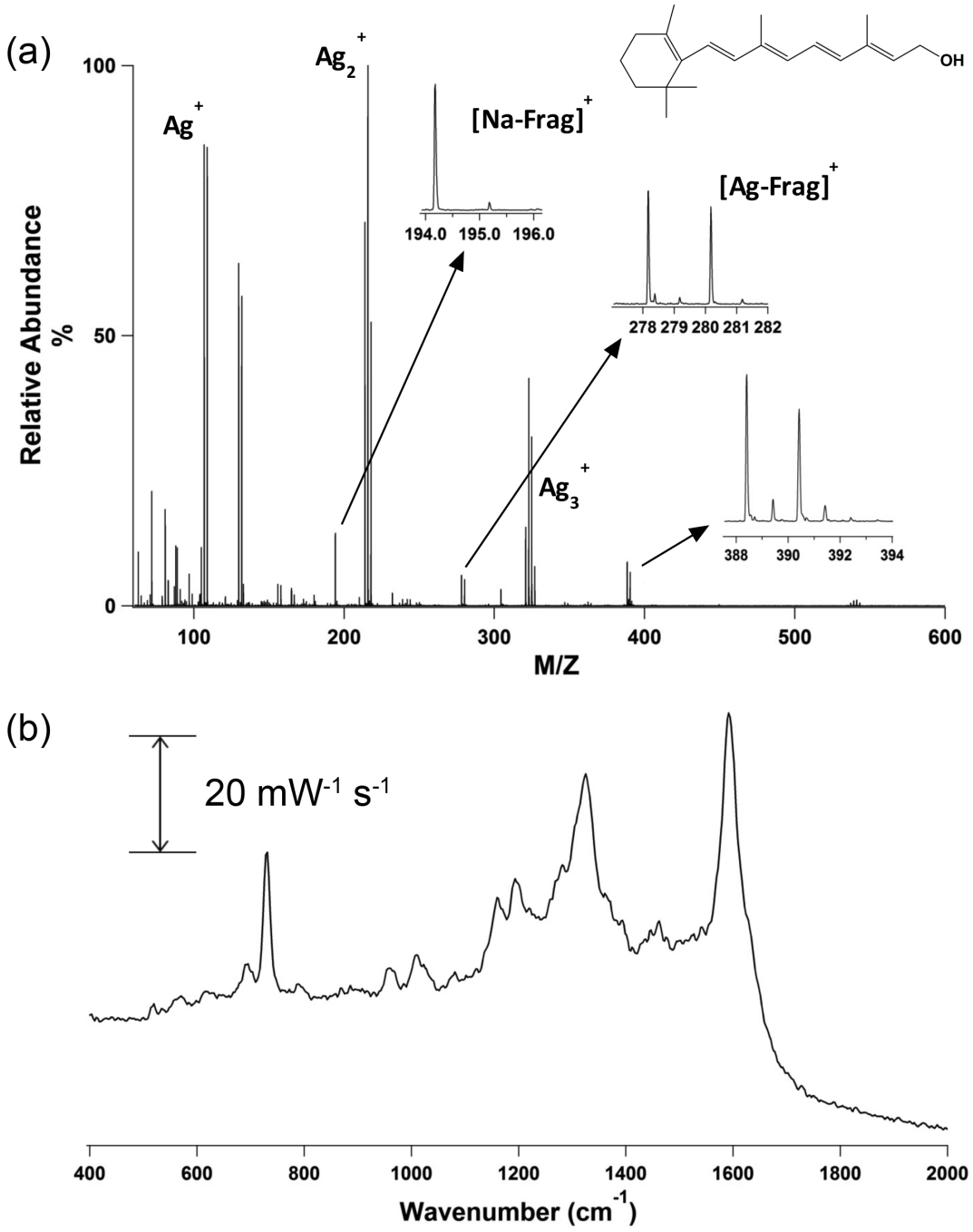

Figure S5. (a) LDI-MS spectrum of retinol (100 picomoles) obtained on 20 nm Ag NP/ITO. (*Insets*) Magnified region near Na and Ag adducts of the same retinol fragment (*m/z* 194.3 and *m/z* 278.3/280.3, respectively). (b) Correlated SERS spectrum of retinol on a Ag NP substrate.

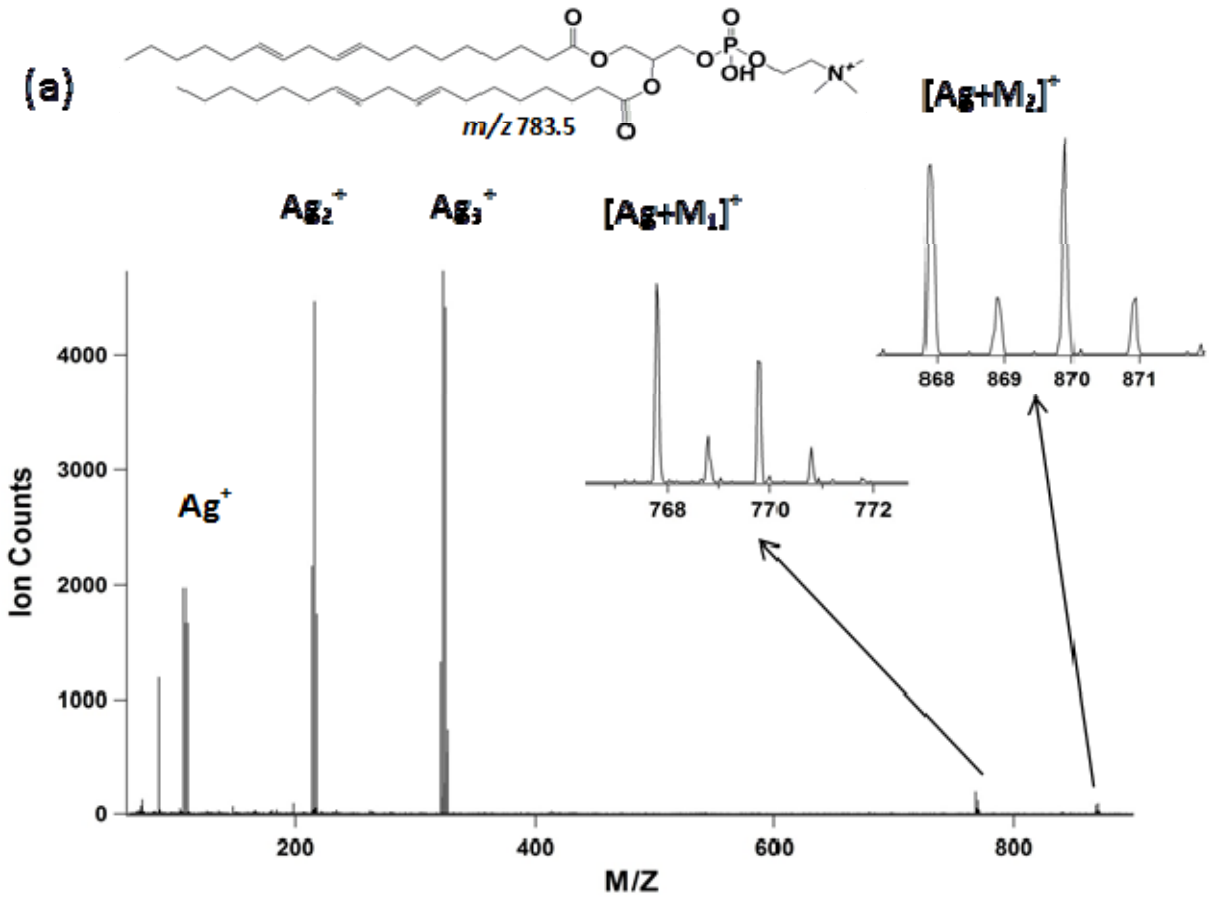
(a)
m/z 783.5
[Ag+M2]+
Ag2+
Ag3+
[Ag+M1]+
Ag+
Ion Counts
M/Z
4000
3000
2000
1000
0
200
400
600
800
868
869
870
871
768
770
772

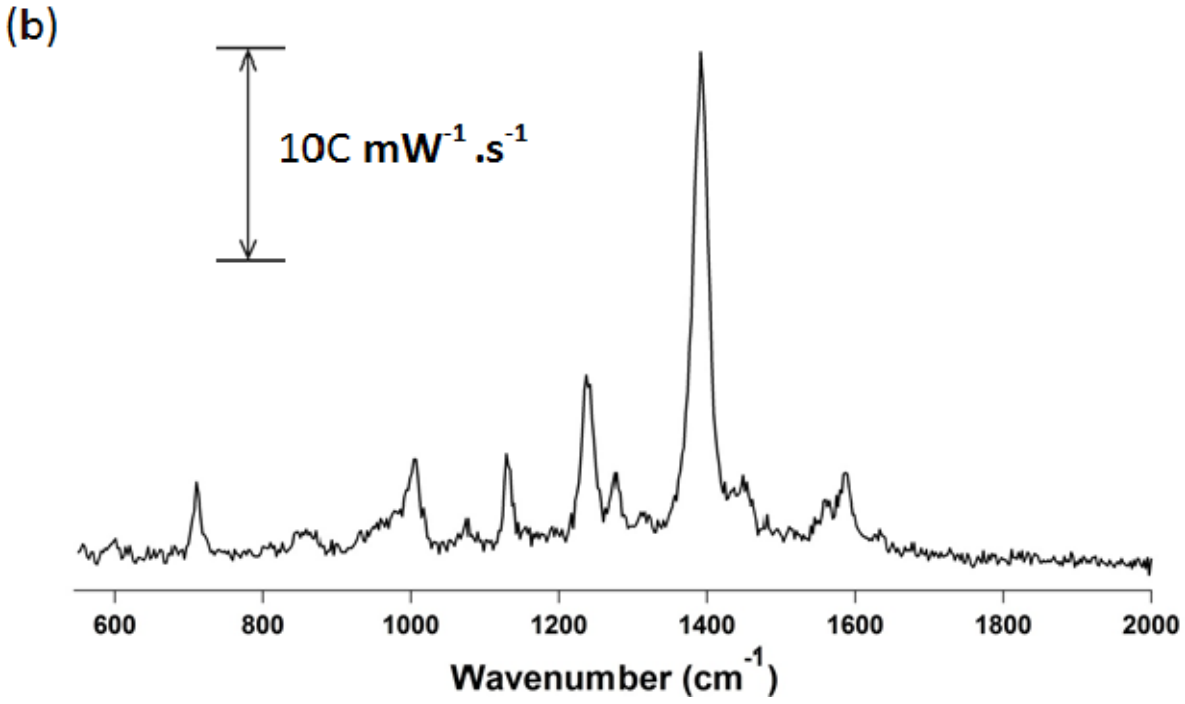
(b)
10C mW-1 .s-1
Wavenumber (cm-1)
600
800
1000
1200
1400
1600
1800
2000

Figure S6. (a) Ag NP LDI mass spectrum of 1,2-dilinoleoyl-*sn*-glycero-3-phosphocholine (*m/z* 783.5). The magnified MS spectra in the insets denoted the Ag adducts with phospholipid fragments (*m/z* 768 and *m/z* 868, respectively). (b) The corresponding SERS spectrum of aforementioned phospholipid deposited onto the same Ag NP substrates.

References

(1) Hu, X.; Cheng, W.; Wang, T.; Wang, Y.; Wang, E.; Dong, S. *Journal of Physical Chemistry B* **2005**, *109*, 19385.

(2) Zheng, J. Z., Y.; Li, X.; Ji, Y.; Lu, T.; Gu, R. *Langmuir* **2003**, *19*, 632.

(3) Baia, M. T., F.; Baia, L.; Popp, J. Astilean, S. *Chem. Phys. Lett.* **2006**, *422*, 127.

(4) Huang, Y. F.; Zhu, H. P.; Liu, G. K.; Wu, D. Y.; Ren, B.; Tian, Z. Q. *J Am Chem Soc* **2010**, *132*, 9244.

(5) Lyandres, O.; Shah, N. C.; Yonzon, C. R.; Walsh, J. T., Jr.; Glucksberg, M. R.; Van Duyne, R. P. *Anal Chem* **2005**, *77*, 6134.

(6) Failloux, N.; Bonnet, I.; Baron, M. H.; Perrier, E. *Appl Spectrosc* **2003**, *57*, 1117.

(7) Leverette, C. L.; Dluhy, R. A. *Colloid Surface A* **2004**, *243*, 157.